Creep and Shrinkage of Self-Compacting Concrete with and without Fibers

Farhad Aslani, Shami Nejadi

Journal of Advanced Concrete Technology, volume 11 (2013), pp. 251-265

Scientific paper

Creep and Shrinkage of Self-Compacting Concrete with and without Fibers

Farhad Aslani[1] and Shami Nejadi[2]

Received 28 November 2012, accepted 18 September 2013 doi:10.3151/jact.11.251

Abstract

Fiber-reinforced self-compacting concrete (FRSCC) is a high-performance building material that combines positive aspects of fresh properties of self-compacting concrete (SCC) with improved characteristics of hardened concrete as a result of fiber addition. Considering these properties, the application ranges of both FRSCC and SCC can be covered. To produce SCC, either the constituent materials or the corresponding mix proportions may notably differ from the conventional concrete (CC). These modifications besides enhance the concrete fresh properties affect the hardened properties of the concrete including creep and shrinkage. Therefore, it is vital to investigate whether all the assumed hypotheses about conventional concrete are also valid for SCC structures. In the present paper, a numerical and experimental study about creep and shrinkage behavior of FRSCC and SCC is performed. Two new creep and shrinkage prediction models based on the comprehensive analysis on the available models of both CC and SCC are proposed for FRSCC and SCC structures. In order to evaluate the predictability of the proposed models, an experimental program was carried out. For this purpose, four SCC mixes - plain SCC, steel, polypropylene, and hybrid FRSCC - are considered in the test program. Several specimens were loaded and deformation in non-loaded specimens was also measured to assess shrinkage. All specimens were kept under constant stress during at least 364 days in a climatic chamber with temperature and relative humidity of 22ºC and 50%, respectively. Results showed that the new models were able to predict deformations with good accuracy, although providing deformations slight overestimated.

1. Introduction

Self-compacting concrete (SCC) can be placed and compacted under its own weight with little or no vibration and without segregation or bleeding. SCC is used to facilitate and ensure proper filling and good structural performance of restricted areas and heavily reinforced structural members. It has gained significant importance in recent years because of its advantages. Recently, this concrete has gained wider use in many countries for different applications and structural configurations. SCC can also provide a better working environment by eliminating the vibration noise. Such concrete requires a high slump that can be achieved by superplasticizer addition to a concrete mix and special attention to the mix proportions. SCC often contains a large quantity of powder materials that are required to maintain sufficient yield value and viscosity of the fresh mix, thus reducing bleeding, segregation, and settlement. As the use of a large quantity of cement increases costs and results in higher temperatures, the use of mineral admixtures such as fly ash, blast furnace slag, or limestone filler could increase the slump of the concrete mix without increasing its cost (Aslani and Nejadi 2012a, 2013).

Fiber-reinforced self-compacting concrete (FRSCC) is a relatively recent composite material that combines the benefits of the SCC technology with the advantages of the fiber addition to a brittle cementitious matrix. It is a ductile material that in its fresh state flows into the interior of the formwork, filling it in a natural manner, passing through the obstacles, and flowing and consolidating under the action of its own weight. FRSCC can mitigate two opposing weaknesses: poor workability in fiber-reinforced concrete (FRC) and cracking resistance in plain concrete. A few studies have been carried out on optimization of the mix proportion for the addition of steel or polypropylene fibers to SCC. Meanwhile, there is insufficient research on the mechanical properties of FRSCC. In mechanical terms, the greatest disadvantage of cementitious material is its vulnerability to cracking, which generally occurs at an early age in concrete structures or members. Cracking may potentially reduce the lifetime of concrete structures and cause serious durability and serviceability problems (Aslani and Nejadi 2012b).

One critical property is creep of concrete. Creep depends on the characteristics of aggregate stiffness and texture, w/c ratio, volume of paste, volume of coarse aggregate, cement type, admixture type, curing method, ratio of volume to surface area, environmental conditions, magnitude of loads and age of loading. According to Neville (1996) mostly the hydrated cement paste experiences creep, while the aggregate is the only portion

[1]Centre for Built Infrastructure Research, School of Civil and Environmental Engineering, University of Technology Sydney, Australia.
E-mail: Farhad.Aslani@uts.edu.au
[2]Centre for Built Infrastructure Research, School of Civil and Environmental Engineering, University of Technology Sydney, Australia.

which resists against creep. Therefore, creep is highly dependent on the stiffness of the chosen aggregate and its proportion within the mixture (Neville 1996). As a result, since creep mainly occurs in the cement paste, main concern arises that SCC may exhibit higher creep because of its high paste content.

Another essential mechanical parameter is the shrinkage of concrete. The overall shrinkage of concrete corresponds to a combination of several shrinkages, that is, plastic shrinkage, autogenous shrinkage, drying shrinkage, thermal shrinkage, and carbonation (chemical) shrinkage. In designing of CC, shrinkage is frequently taken as drying shrinkage, which is the strain associated with the loss of moisture from the concrete under drying conditions, because with a relatively high water-to-cementitious material ratio (w/c) (higher than 0.40) CC exhibits a relatively low autogenous shrinkage $<100\times10^{-6}$ (Aslani and Nejadi 2011a). In contrast, the SCC used in the precast industry, namely for prestressed applications, has typically a low w/c ratio (0.32 to 0.40). These relatively low w/c ratios, coupled with a high content of binder lead to greater autogenous shrinkage. Such shrinkage increases and is notable in SCC because of the use of finely ground supplementary cementitious materials and fillers. Therefore, both drying and autogenous shrinkage deformations have to be accounted in the structural detailing of reinforced concrete and prestressed concrete members (Khayat and Long 2010).

Being aware that SCC usually has higher paste volume and/or higher sand-to-aggregate ratio to achieve high workability, several researchers have claimed relatively large creep and shrinkage of SCC for precast/prestressed concrete, resulting in larger prestress losse. In fact, although mechanical properties of SCC are superior to those of CC, creep and shrinkage of SCC are significantly high (Issa *et al*. 2005). Among others, Naito *et al*. (2006) also found that SCC exhibits higher shrinkage and creep than CC, which is due probably to the high fine aggregate and paste volume in the SCC.

On the other hand, Schindler *et al*. (2007) revealed that the shrinkage of SCC is similar or less than that of CC. When the shrinkage of SCC is compared to that of CC at 112 days, the sand-to-aggregate ratio effect is not significant for the shrinkage of SCC. The creep coefficients of SCC mixtures were also smaller than those of CC at all loading ages. This was attributed to the low w/c.

The different methodology followed to obtain SCC in different countries and the limited number of studies concerning its long-term behavior make still not clear if current International Standards can be applied successfully also for SCC. Moreover, it is not even assessed if long-term properties can be predicted with reference to conventional mechanical and physical parameters only (like strength or w/c) or the adoption of parameters concerning the mix design is needed.

2. Research significance

It is vital to investigate whether all the assumed hypotheses used to design structures of conventional concrete about creep and shrinkage are also valid for FRSCC and SCC structures. Thus, the objectives of this study are:

(a) To review the accuracies of the CC creep and shrinkage prediction models proposed by international codes of practice, including CEB-FIP (2010), ACI 209R (1997), Eurocode 2 (2004), JSCE (2002), AASHTO (2004; 2007) and AS 3600 (2009).
(b) To review the accuracies of the SCC creep and shrinkage prediction models proposed by Poppe and De Schutter (2005), Larson (2007), Cordoba (2007) and Khayat and Long (2010).
(c) To propose a new prediction creep and shrinkage model based on the comprehensive analysis of the available models and the experimental results database of both the CC and the FRSCC & SCC.
(d) To verify the predictability of the proposed models on experimental results conducted in a mix composition previously used in the prefabrication of prestressed bridge girders, i.e. a FRSCC & SCC loaded at early ages.

3. Experimental program

An experimental program with shrinkage and creep tests was carried out in laboratory. For this purpose, four SCC mixes - plain SCC, steel, polypropylene, and hybrid FRSCC - are considered in the test program. Several specimens were loaded and deformation in non-loaded specimens was also measured to assess shrinkage. All specimens were kept under constant stress during at least 364 days in a climatic chamber.

3.1 Materials

3.1.1 Cement

In this experimental study, shrinkage limited cement (SLC) corresponding to the ASTM C183-08 (2000) (AS 3972, 2010) standard was used. SLC is manufactured from specially prepared portland cement clinker and gypsum. It may contain up to 5% of AS 3972 approved additions. The chemical, physical, and mechanical properties of the cement used in the experiments are shown in **Table 1**. The chemical, physical, and mechanical properties adhere to the limiting value or permissible limits specified in AS 2350.2, 3, 4, 5, 8, and 11 (2006).

3.1.2 Fly ash

It is important to increase the amount of paste in SCC because fly ash is an agent to carry the aggregates. Erarring fly ash (EFA) is a natural pozzolan. It is a fine cream/grey powder that is low in lime content. The chemical and physical properties of EFA used in the experimental study are given in **Table 1**. The chemical,

Table 1 Properties of cement, fly ash, and ground granulated blast furnace slag (GGBFS).

Cement		Fly Ash		GGBFS	
Chemical properties		Chemical properties		Chemical properties	
CaO	64.5 %	Al_2O_3	26.40 %	Al_2O_3	14.30 %
SiO_2	19.3 %	CaO	2.40 %	Fe_2O_3	1.20 %
Al_2O_3	5.2 %	Fe_2O_3	3.20 %	MgO	5.40 %
Fe_2O_3	2.9 %	K_2O	1.55 %	Mn_2O_3	1.50 %
MgO	1.1 %	MgO	0.60 %	SO_3	0.20 %
SO_3	2.9 %	Mn_2O_3	<0.1 %	Cl	0.01 %
K_2O	0.56 %	Na_2O	0.47 %	Insoluble Residue	0.50 %
Na_2O	<0.01 %	P_2O_5	0.20 %	LOI	-1.10 %
Cl	0.02 %	SiO_2	61.40 %	Physical properties	
LOI	2.8 %	SO_3	0.20 %	Fineness Index	435 m^2/kg
Physical properties		SrO	<0.1 %		
Autoclave Expansion	TiO_2	TiO_2	1.00 %		
Fineness Index	405 m^2/kg	Physical properties			
Mechanical properties		Moisture	<0.1 %		
Initial Setting Time	90 mins	Fineness 45 micron	78% passed		
Final Setting Time	135 mins	Loss on Ignition	2.30 %		
Soundness	1.0 mm	Sulfuric Anhydride	0.20 %		
Drying Shrinkage	590 μstrain	Alkali Content	0.50 %		
f'_c (3 Days)	37.2 MPa	Chloride Ion	<0.001 %		
f'_c (7 Days)	47.3 MPa	Relative Density	2.02 %		
f'_c (28 Days)	60.8 MPa	Relative Water Requirement	97 %		
		Relative Strength 28 Days	88 %		

physical, and mechanical properties of the EFA used adhere to the limiting value or permissible limits specified in ASTM C311-11b (2000) (ACI 232.2R-03, 2004; AS 2350.2, 2006; AS 3583.1, 2, 3, 5, 6, 12, and 13, 1998).

3.1.3 Ground granulated blast furnace slag

Granulated blast furnace slag (GGBFS) is another supplementary cementitious material that is used in combination with SLC. GGBFS used in the experiment originated in Boral, Sydney, and it conformed to ASTM C989-06 (2000) (ACI 233R-95, 2000; AS 3582.2, 2001) specifications. The chemical and physical properties of GGBFS are given in **Table 1**.

3.1.4 Aggregate

In this study, crushed volcanic rock (i.e., latite) coarse aggregate was used with a maximum aggregate size of 10 mm. Nepean river gravel with a maximum size of 5 mm and Kurnell natural river sand fine aggregates were also used. The sampling and testing of aggregates were carried out in accordance with ASTM C1077-13 (2000) (AS 1141, 2011; RTA 2006) and the results for coarse and fine aggregates are shown in **Tables 2**, respectively.

3.1.5 Admixtures

The superplasticiser, viscosity-modifying admixture (VMA), and high-range water-reducing agent were used in this study. The new superplasticiser generation Glenium 27 complies with AS 1478.1 (2000) type High Range Water Reducer (HRWR) and ASTM C494 (2000) types A and F are used. The Rheomac VMA 362 viscosity modifying admixture that used in this study is a ready-to-use, liquid admixture that is specially developed for producing concrete with enhanced viscosity and controlled rheological properties. Pozzolith 80 was used as a high-range water-reducing agent in the mixes. It meets AS 1478 (2000) Type WRRe, requirements for admixtures.

3.1.6 Fibers

In this study, two commercially available fibers, Dramix RC-80/60-BN type steel fibers and Synmix 65 type polypropylene (PP) fibers were used. The mechanical, elastic and surface structure properties of the steel and PP fibers are summarized in **Table 3**.

3.2 Mixture proportions

One control SCC mixture (N-SCC) and three fiber-reinforced SCC mixtures were used in this study. Fiber-reinforced SCC mixtures contain steel (D-SCC), PP (S-SCC), and hybrid (steel + PP) (DS-SCC) fibers. The content proportions of these mixtures are given in **Table 4**. These contents were chosen to attempt to keep compressive strength to a level applicable to construction. As shown in **Table 4**, cement, fly ash, GGBFS, water, fine and coarse aggregates, VMA, and high range water reducing agent constituents amount are same for four mixes. But, fiber amount and superplasticiser that are used in the mixes are different.

A forced pan type of mixer with a maximum capacity of 150 liters was used. The volume of a batch with fibers was kept constant at 50 liters. First, powders and sand are mixed for 10 s and water and superplasticiser are added and mixed for 110 s and the coarse aggregate

Table 2 Properties of crushed latite volcanic rock coarse aggregate, Nepean river gravel fine aggregate, and Kurnell natural river sand fine aggregate.

Crushed latite volcanic rock coarse aggregate		Nepean river gravel fine aggregate		Kurnell natural river sand fine aggregate	
Characteristics	Results	Characteristics	Results	Characteristics	Results
Sieve size	Passing (%)	Sieve size	Passing (%)	Sieve size	Passing (%)
13.2 mm	100	6.7 mm	100	1.18 mm	100
9.5 mm	89	4.75 mm	99	600 micron	98
6.7 mm	40	2.36 mm	83	425 micron	87
4.75 mm	7	1.18 mm	64	300 micron	46
2.36 mm	1	600 micron	42	150 micron	1
1.18 mm	1	425 micron	28	Material finer than 75 micron in aggregate by washing (%)	Nil
Material finer than 75 micron (%)	1	300 micron	19	Uncompacted Bulk Density (t/m^3)	1.39
Mis-shapen particles (%)		150 micron	8	Compacted Bulk Density (t/m^3)	1.54
Ratio 2:1	13	Material finer than 75 micron (%)	3	Particle Density (Dry) (t/m^3)	2.58
Ratio 3:1	1	Uncompacted Bulk Density (t/m^3)	1.52	Particle Density (SSD) (t/m^3)	2.59
Flakiness Index (%)	20	Compacted Bulk Density (t/m^3)	1.64	Apparent Particle Density (t/m^3)	2.62
Uncompacted Bulk Density (t/m^3)	1.36	Particle Density (Dry) (t/m^3)	2.58	Water Absorption (%)	0.6
Compacted Bulk Density t/m^3	1.54	Particle Density (SSD) (t/m^3)	2.60	Silt Content (%)	4
Moisture condition of the aggregate (%)	1.3	Apparent Particle Density (t/m^3)	2.63		
Particle Density (Dry) (t/m^3)	2.65	Water Absorption (%)	0.7		
Particle Density (SSD) (t/m^3)	2.70	Silt Content (%)	7		
Apparent Particle Density (t/m^3)	2.79	Degradation Factor of Fine Aggregate The wash water after using permitted 500ml was: CLEAR	90		
Water Absorption (%)	1.9	Moisture Content (%)	5.5		
Ave. Dry Strength (kN)	391	Method of Determining Voids Content			
Ave. Wet Strength (kN)	293	% Voids	41.7		
Wet/Dry Strength Variation (%)	25	The mean Flow Time (Sec.)	26.5		
Test fraction (mm)	-9.5+6.7				
The amount of significant breakdown (%) The size of testing cylinder = 150 mm diam.	<0.2				
Los Angeles Value Grd. 'K' (%Loss)	13				

is added and at the end fibers are added to the pan and mixed for 90 s.

3.3 Samples' preparation and curing conditions

We used three ϕ100 mm × 200 mm molds for the determination of compressive strength at age 28 days and three cylindrical molds ϕ100 mm × 200 mm are used for the determination of the modulus of elasticity. Specimens for testing the hardened properties are prepared by direct pouring of concrete into molds without compaction. The specimens are kept covered in a controlled chamber at 20 ± 2℃ for 24 h until demolding. Thereafter, the specimens are placed in water presaturated with lime at 20℃. These specimens are tested at. For each test, separated specimens are used and surface of specimens are smoothed.

Three 75 mm × 75 mm × 280 mm molds are used for the determination of drying shrinkage. After demolding shrinkage specimens, all of them are stored in standard temperate moist curing conditions at the measuring laboratory for a minimum of 24 h prior to initial measurement. Five ϕ100 mm × 200 mm cylinders are used for the determination of creep in one creep rig. The applied stress value was determined by the 40% of the 28

Table 3 The physical and mechanical properties of fibers.

Fibre type	Fibre name	Density (kg/m^3)	Length (l)	Diameter (d)	Aspect ratio (l/d)	Tensile strength (MPa)	Modulus of elasticity (GPa)	Cross-section form	Surface structure
Steel	Dramix RC-80/60-BN	7850	60	0.75	80.0	1050	200	Circular	Hooked end
Polipropylene (PP)	Synmix 65	905	65	0.85	76.5	250	3	Square	Rough

Table 4 The proportions of the concrete mixtures (based on SSD condition).

Constituents	N-SCC	D-SCC	S-SCC	DS-SCC
Cement (kg/m^3)	160	160	160	160
Fly Ash (kg/m^3)	130	130	130	130
GGBFS (kg/m^3)	110	110	110	110
Cementitious content (kg/m^3)	400	400	400	400
Water (lit/m^3)	208	208	208	208
Water cementitious Ratio	0.52	0.52	0.52	0.52
Fine aggregate (kg/m^3)				
Coarse Sand	660	660	660	660
Fine Sand	221	221	221	221
Coarse aggregate (kg/m^3)	820	820	820	820
Admixtures (lit/m^3)				
Superplasticiser	4	4.86	4.73	4.5
VMA	1.3	1.3	1.3	1.3
High range water reducing agent	1.6	1.6	1.6	1.6
Fibre content (kg/m^3)				
Steel	-	30	-	15
PP	-	-	5	3

days compressive strength results. All shrinkage and creep specimens are hold in the drying room with suitably controlled temperature, humidity and air circulation. The temperature and relative humidity of the drying room was 23±2ºC and 50±5% respectively.

3.4 Samples' test methods

The compressive strength test, performed on ϕ100 mm × 200 mm cylinders, followed AS 1012.14 (1991) and ASTM C39 (2000) tests for compressive strength of cylindrical concrete specimens. The cylinders were loaded in a testing machine under load control at the rate of 0.3 MPa/s until failure. The modulus of elasticity test that followed the AS 1012.17 (1997) and ASTM C469 was done to ϕ100 mm × 200 mm cylinders.

The shrinkage test, performed on 75 mm × 75 mm × 280 mm prisms, followed AS 1012.13 (1992) determination of the drying shrinkage of concrete test method. The creep test is performed on five ϕ100 mm × 200 mm cylinders in one creep rig, followed AS 1012.16 (1996) determination of creep of concrete cylinders in compression test method.

3.5 Properties of fresh concrete

The experiments required for the SCC are generally carried out worldwide under laboratory conditions. These experiments test the liquidity, segregation, placement, and compacting of fresh concrete. Conventional workability experiments are not sufficient for the evaluation of SCC. Some of the experiment methods developed to measure the liquidity, segregation, placement, and compaction of SCC are defined in the European guidelines (2005) and ACI 237R-07 (2007) for SCC, including specification, production and use as slump–flow, V-funnel, U-box, L-box and fill-box tests.

This study performed slump flow, T_{50cm} time, J-ring flow, V-funnel flow time, and L-box blocking ratio tests. In order to reduce the effect of loss of workability on the variability of test results, the fresh properties of the mixes were determined within 30 min after mixing. The order of testing is as follows: 1. Slump flow test and measurement of T_{50cm} time; 2. J-ring flow test, measurement of difference in height of concrete inside and outside the J-ring and measurement of T_{50cm} time; 3. V-funnel flow tests at 10 s T_{10s} and 5 min T_{5min}; and 4. L-box test.

4. Experimental results

4.1 Properties of fresh concrete

The results of various fresh properties tested by the slump flow test (slump flow diameter and T_{50cm}); J-ring test (flow diameter); L-box test (time taken to reach 400 mm distance T_{400mm}, time taken to reach 600 mm distance T_{600mm}, time taken to reach 800 mm distance T_L, and ratio of heights at the two edges of L-box [H_2/H_1]); V-funnel test (time taken by concrete to flow through V-funnel after 10 s T_{10s}); the amount of entrapped air; and the specific gravity of mixes are given in **Table 5**. The slump flow test judges the capability of concrete to deform under its own weight against the friction of the surface with no restraint present. A slump flow value

Table 5 The SCC mixes workability characteristics.

Workability characteristics	N-SCC	D-SCC	S-SCC	DS-SCC
Average spreading diameter (mm)	680	670	700	650
Flow time T_{50cm} (s)	2.7	3.8	2.5	3.2
Average J-Ring diameter (mm)	655	580	570	560
Flow time T_{50cm} J-Ring (s)	3.2	5	6	5
L-box test	0.87	Blocked*	Blocked	Blocked
Flow time V-funnel (s)	6	7	Blocked	Blocked
V-funnel at $T_{5minutes}$ (s)	4	5	Blocked	Blocked
Entrapped air (%)	1.3	1.2	1.2	1.0
Specific gravity (kg/m^3)	2340	2274	2330	2385

* Fibers are the main reason for blockage.

Table 6 The experimental result of compressive strength and modulus of elasticity of SCC mixes.

	N-SCC	D-SCC	S-SCC	DS-SCC
Compressive strength (MPa)	33.60	38.30	33.00	42.00
Modulus of Elasticity (MPa)	3599	3870	3424	3771

ranging from 500 to 700 mm for self-compacting concrete was suggested (European guidelines, 2005). At a slump flow > 700 mm the concrete might segregate, and at <500 mm, the concrete might have insufficient flow to pass through highly congested reinforcements. All the mixes in the present study conform to the above range, because the slump flow of SCC is in the range of 600–700 mm. The slump flow time for the concrete to reach a diameter of 500 mm for all mixes was less than 4.5 s. The J-ring diameters were in the range of 560–655 mm. In addition to the slump flow test, a V-funnel test was also performed to assess the flowability and stability of SCC. V-funnel flow time is the elapsed time in seconds between the opening of the bottom outlet, depending when it is opened (T_{10s} and T_{5min}), and the time when light becomes visible at the bottom when observed from the top. According to the European guidelines (2005), a period ranging from 6 to 12 s is considered adequate for SCC. The V-funnel flow times in the experiment were in the range of 7–11 s. The test results of this investigation indicated that all mixes met the requirements of allowable flow time. About V-funnel flow time test results for the N-SCC mix was 6 s and for the D-SCC was 7 s and for other fiber reinforced SCC mixes are blocked, obviously.

The maximum size of coarse aggregate was restricted to 10 mm to avoid a blocking effect in the L-box for N-SCC mix. The gap between rebars in the L-box test was 35 mm. The L-box ratio H_2/H_1 for the N-SCC mix was above 0.8 which is, according to the European guidelines and, obviously, for other mixes is blocked. A total spread over 700 mm was measured and no sign of segregation or considerable bleeding in any of the mixtures was detected as the mixtures showed good homogeneity and cohesion.

4.2 Compressive strength and modulus of elasticity

Table 6 presents the average compressive strength and modulus of elasticity of N-SCC, D-SCC, S-SCC, and DS-SCC mixes.

4.3 Deformation measurements results

Results of the shrinkage strain, creep strain, and total strain for all sets of loaded specimens are presented in **Figs. 1-3** and **Table 7**. After the commencement of drying, the shrinkage strain developed rapidly within the first two or three months and more than 50% of shrinkage occurred during this period. The maximum measured final shrinkage strain or N-SCC, D-SCC, S-SCC, and DS-SCC, and N-CC mixtures were 870, 844, 823, and 882 microstrains after 364 days. The maximum measured final shrinkage strain for SCC mixtures are not much different from each other.

The creep strains increased quickly for the first few weeks after loading, with almost 50% of creep occurring in the first 40 days after loading. The final creep strains for N-SCC, D-SCC, S-SCC, DS-SCC, and N-CC mixtures were 1773, 1686, 1997, and 1736 microstrains after 364 days. There are very interesting results here the creep coefficient of DS-SCC mixture has same trend like N-CC. But, the other SCC mixtures have different behavior. The maximum creep coefficient is related to S-SCC with PP fibers in the mixture. The creep coefficient of S-SCC mixture at age 364 days is 11%, 15%, and 13% higher than N-SCC, D-SCC, and DS-SCC mixtures, respectively.

5. Numerical analysis

Based on the recent studies of Aslani and Nejadi (2011 a,b) following procedure are used for comparing available conventional concrete creep and shrinkage models: 1. Establish an experimental database for creep and shrinkage results. 2. Establish creep and shrinkage available prediction models database. 3. Comparing creep and shrinkage models with SCC experimental results database. 4. Proposing SCC creep and shrinkage models based on the pervious comparisons. 5. Verification of proposed SCC creep and shrinkage models with

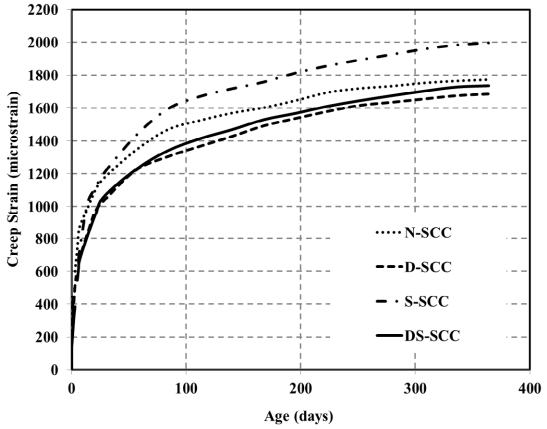

Fig. 1 Creep strain for all specimens loaded.

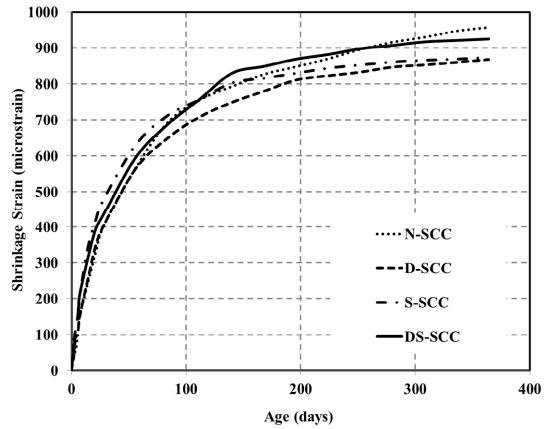

Fig. 2 Shrinkage strain for all specimens.

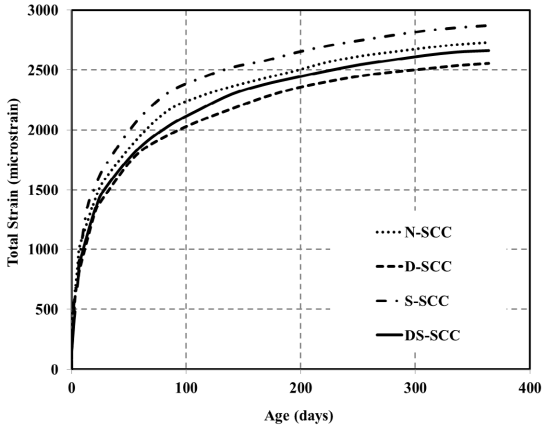

Fig. 3 Total strain for all specimens loaded.

experimental results tests that have been done in this study.

5.1 Creep and shrinkage experimental results database

Tables 8-9 present a general summary of the creep and shrinkage concrete mixtures included in the database. The database comprises test results from 11 different investigations, with a total of 52 SCC and 11 CC mixtures for creep tests. Also, the database comprises test results from 14 different investigations, with a total of 165 different SCC mixtures and 21 CC mixtures for shrinkage tests. **Tables 8-9** also include complimentary information regarding the applied stress to the creep specimens, age of concrete when shrinkage begins (days), final age of the concrete, relative humidity (*RH*), type of the specimen, type of the cement and filler.

5.2 Creep and shrinkage models

This paper also, assesses the accuracy of seven commonly used international code type models that are used to predict creep and shrinkage strains. These empirically based models, which vary widely in their techniques, require certain intrinsic and/or extrinsic variables, such as mix proportions, material properties and age of loading as input. The models considered are listed in **Table 10**, which also shows the factors accounted by each model. In this study the accuracy of the creep and shrinkage prediction models proposed by international codes of practice, including: CEB-FIP (2010), ACI 209R (1997), Eurocode 2 (2004), JSCE (2002), AASHTO (2004), AASHTO (2007) and AS 3600 (2009) are compared with the actual measured creep and shrinkage strains.

As shown in the **Table 11**, the AASHTO (2007), JSCE (2002), Eurocode 2 (2004) and AASHTO (2004) models provided better prediction of creep data for CC mixture in the experimental database with a coefficient of correlation factor (R^2) of 0.90, 0.89,0.89 and 0.86 compared to other models. Also, as shown in the **Table 11**, for SCC mixture in the experimental database, AASHTO (2004), JSCE (2002) and ACI 209R (1992) models provided better prediction of creep data with a coefficient of correlation factor (R^2) of 0.87, 0.87 and 0.84 compared to other models.

AASHTO (2004), JSCE (2002) and ACI 209R (1992) CC creep models that have conservative predictions for SCC mixtures in the database are different in the certain intrinsic and/or extrinsic variables. As mentioned in the **Table 11**, the AASHTO (2004) creep model has not any intrinsic factors but the JSCE (2002) and ACI 209R (1992) creep models have a good consideration of both intrinsic variables (i.e. aggregate type, aggregates/cement ratio, air content, cement content, cement type, concrete density, fine/total aggregate ratio, slump, w/c ratio, and water content) and extrinsic variables (i.e. age at the first loading, age of sample, applied stress, characteristic strength at loading, cross-section shape, curing conditions, compressive strength at 28 days, duration of load, effective thickness, elastic modulus at age of loading, elastic modulus at 28 days, relative humidity, temperature, and time drying commences). The modified composition of SCC in comparison with CC influences the creep behavior of the concrete. Therefore, it is important to include some important variables that have impact on this behavior. By consideration these variables, JSCE (2002) creep model have good intrinsic and extrinsic variables.

Table 7 The experimental result of shrinkage and creep strains of SCC mixes.

Time	N-SCC		D-SCC		S-SCC		DS-SCC	
	shrinkage (μm)	creep (μm)	shrinkage (μm)	creep (μm)	shrinkage (μm)	creep (μm)	shrinkage (μm)	creep (μm)
0hr	0	0	0	0	0	0	0	0
2hr	0	311	3	117	11	104	10	116
6hr	1	393	8	182	17	202	10	148
1d	12	479	22	309	42	389	36	220
2d	*	*	42	412	79	459	64	316
3d	52	601	81	515	105	518	95	385
4d	64	672	98	571	134	569	*	*
5d	91	742	*	*	*	*	142	545
6d	121	827	119	654	166	671	172	610
7d	150	872	150	680	204	730	210	670
14d	242	991	251	835	339	1024	310	819
21d	329	1105	348	974	419	1116	394	951
28d	403	1172	404	1035	479	1202	436	1060
56d	567	1344	565	1222	631	1432	596	1226
84d	693	1469	650	1305	713	1595	688	1341
112d	756	1525	709	1368	757	1671	758	1414
140d	793	1570	749	1428	803	1718	830	1469
168d	827	1603	780	1493	816	1759	849	1530
196d	848	1647	811	1538	830	1815	869	1569
224d	870	1696	823	1581	844	1858	882	1612
252d	896	1720	833	1617	853	1894	898	1646
280d	916	1734	847	1636	861	1927	907	1676
308d	930	1753	853	1656	866	1960	917	1704
336d	947	1765	860	1676	869	1984	921	1728
364d	957	1773	868	1686	874	1997	925	1736

As show in the **Table 12**, for CC mixture in the experimental database, the AASHTO (2007) and JSCE (2002) models provided a better prediction of drying shrinkage data with a coefficient of correlation factor (R^2) of 0.88 and 0.84 compared to other models. Also, as shown in the **Table 12**, the AASHTO (2007), JSCE (2002) and AS 3600 (2009) models provided a better prediction of SCC mixture in the experimental database drying shrinkage data with a coefficient of correlation factor (R^2) of 0.86, 0.83 and 0.80 compared to compared to other models.

The CC shrinkage models of AASHTO (2007) and JSCE (2002) that have conservative predictions for SCC mixtures in the database are different in the certain intrinsic and/or extrinsic variables. As mentioned in the **Table 10**, the AASHTO (2007) shrinkage model has not any intrinsic factors but the JSCE (2002) shrinkage model has a good consideration of both intrinsic and extrinsic variables. When compared to the CC, the modified composition of SCC has influence in the shrinkage behavior of concrete. Therefore, it is important to involve some important variables that have impact on this behavior. By consideration these variables, JSCE (2002) shrinkage model have good intrinsic and extrinsic variables.

5.3 Proposed creep model

The comparison of the different models and the experimental database shows that ACI 209R (1997), JSCE (2002) and AASHTO (2004) models have conservative creep coefficient predictions. In this study, based on required certain intrinsic and/or extrinsic variables for SCC, JSCE (2002) creep model gives the good approximation of the creep coefficient. Therefore, with the JSCE (2002) creep model as a basis, it is tried to formulate some suggestions to include the c/p (cement-to-powder) ratio into the formulas in order to obtain a better prediction of the time-dependent deformations of normal strength and high strength of SCC. These results are showed into Eq. (1) to Eq. (10).

A) For the normal strength SCC with range of applicability (see the denomination of the parameters in the Notation Section):

$$45\% \le RH \le 80\%\,;120kg/m^3 \le w \le 230kg/m^3\,;$$
$$100mm \le v/s \le 300mm\,;0.30 \le w/c \le 0.65\,;$$
$$f_{c,28d} \le 55MPa\,;260kg/m^3 \le c \le 500kg/m^3\,.$$

$$\varepsilon'_{cc}(t,t',t_0) = \sigma'_{cp} \times \varepsilon'_{cr}\left[1-\exp\left\{-0.09(t-t')^{0.54}\right\}\right] \times (0.015+1.35(c/p))^{-1} \quad for \quad c/p < 0.65 \tag{1}$$

$$\varepsilon'_{cc}(t,t',t_0) = \sigma'_{cp} \times \varepsilon'_{cr}\left[1-\exp\left\{-0.09(t-t')^{0.54}\right\}\right] \times (0.015+1.05(c/p))^{-1} \quad for \quad c/p < 0.65 \tag{2}$$

$$\sigma'_{cp} = \frac{\mu + \lambda.\sigma(t,t_0)^{\alpha}}{1-\kappa} \quad \text{non-linear creep amplification function} \tag{3}$$

where μ and λ and α are additional parameters to be obtained from a least square minimization procedure starting from experimental data $\mu=0.90$, $\lambda=1.80$, $\alpha=2.10$; moreover, the stress function $\sigma(t, t_0)$ is the actual stress/strength ratio, being:

Table 8 Creep experimental results database.

Reference	No. of SCC mixtures	No. of CC mixtures	Applied stress to the creep specimens	Final age of concrete (days)	R.H. (%)	Type of specimen (mm)	Type of cement	Type of Filler
Chopin *et al.* (2003)	5	1	40% or 60% of the compressive strength at 28 days	365	50	Cylinder (90 × 280)	CEM I	Limestone
Poppe and De Schutter (2005)	6	0	1/3 of the compressive strength at 28 days	1400	60	Prism (150×150×500)	CEM I 42.5 R, CEM I 52.5	Limestone
Horta (2005)	6	0	40% of the compressive strength at 28 days	70, 200	50	Cylinder (150 × 300)	CEM I , CEM III	Fly ash and GGBFS
Larson (2006)	1	0	40% of the compressive strength at 28 days	520	50	Prism (101.6×101.6×609.6) and Cylinder (114.3×609.6)	CEM III	Limestone
Turcry *et al.* (2006)	3	3	20% of the compressive strength at 7 days	65, 100	50	Cylinder (110 x 200)	CEM I 52.5, CEM II 42.5	Limestone
Cordoba (2007)	4	1	30% of the compressive strength at 28 days	365	50	Cylinder (101.6 × 203.2), (101.6 × 1057.8)	CEM I/II	Fly ash and GGBFS
Heirman *et al.* (2008)	7	1	±1/3 of the compressive strength at 28 days	70	60	Cylinder (120 × 300)	CEM I 42.5 R, CEM III/A 42.5 N LA	Limestone
Oliva and Cramer (2008)	11	4	40% of the compressive strength at 28 days	495	50	Cylinder (152.4 × 213.6)	CEM I	GGBFS
Kim (2008)	4	4	Changeable for each mixture	150	50	Cylinder (100×200)	CEM III	Fly ash and Limestone
Zheng *et al.* (2009)	7	1	30% of the compressive strength at loading days	150	60	Prism (100×100×400)	CEM I	Fly ash
Loser and Leemann (2009)	1	1	Changeable for each mixture	91	70	Prism (120×120×360)	CEM I 42.5 N, CEM II/A-LL 45.2 N	Fly ash and Limestone
Total of 71 mixtures	55	16						

Table 9 Shrinkage experimental results database.

Reference	No. of SCC mixtures	No. of CC mixtures	Age of concrete when shrinkage begins (days)	Final age of concrete (days)	R.H. (%)	Type of specimen (mm)	Type of cement	Type of filler
Chopin *et al.* (2003)	5	1	1	365	50	Cylinder (90 × 280)	CEM I	Limestone
Poppe and De Schutter (2005)	4	0	1	1400	60	Prism (150×150×500)	CEM I 42, 5 R, CEM I 52,5	Limestone
Horta (2005)	6	0	1	200	50	Cylinder (150 × 300)	CEM I , CEM III	Fly ash and GGBFS
Larson (2006)	1	0	1	520	50	Prism (101.6×101.6×609.6) and Cylinder (114.3×609.6)	CEM III	Limestone
Turcry *et al.* (2006)	3	3	1	120, 150, 210	50	Prism (70×70×280)	CEM I 52.5, CEM II 42.5	Limestone
Cordoba (2007)	4	1	1	365	50	Cylinder (101.6 × 203.2), (101.6 × 1057.8)	CEM I/II	Fly ash and GGBFS
Heirman *et al.* (2008)	7	1	1	98	60	Cylinder (120 x 300)	CEM I 42.5 R, CEM III/A 42.5 N LA	Limestone
Bhattacharya (2008)	6	2	1	90	50	Prism (76.2×76.2×311.2)	CEM I	Limestone, Silica fume and Slag
Oliva and Cramer (2008)	11	4	1	350, 495	50	Prism (101.6×101.6×285.75)	CEM I	GGBFS
Hwang and Khayat (2009)	10	2	1	56	50	Prism (75x75×285)	CSA type Gub-F/SF, Gub-S/SF and quaternary blended cement	Fly ash and Limestone
Ma *et al.* (2009)	16	0	1	120, 150	60	Prism (100×100×515)	CEM I	Fly ash
Loser and Leemann (2009)	13	3	1	91	70	Prism (120×120×360)	CEM I 42.5 N, CEM II/A-LL 45.2 N	Fly ash and Silica fume
Güneyisi *et al.* (2010)	63	2	1	50	50	Prism (70×70×280)	CEM I	Fly ash, GGBFS, Silica fume and Metakaolin
Khayat and Long (2010)	16	2	1	300	50	Cylinder (150×300)	MS and HE (similar to ASTM C150 Type I/II and Type III)	Fly ash
Total of 186 mixtures	165	21						

$$\sigma(t,t_0)=\frac{\sigma(t_0)}{f_{cm}(t)} \tag{4}$$

in the case of constant applied load. In Eq. (3), numerator and denominator indicate the effect of sustained load and the effect of a damage level due to instantaneous loading. The law $f_{cm}(t)$ representing the evolution with time of compression strength has been defined by modifying MC90 proposal according to expression:

$$f_{cm}(t)=f'_{c,28}.\exp\left[s'\left(1-\left(\frac{28}{t}\right)^{n}\right)\right] \tag{5}$$

where parameters s' and n have been specifically calibrated for each SCC concrete mix by using experimental results previously described. According to the available data, parameters s' and n range from 0.2–0.6, and 0.28–0.35, respectively. The adoption of function $\sigma(t, t_0)$ allows for variable rate of increase of mechanical properties be taken into account, particularly important for concretes loaded at early ages. Finally, the non-linear behavior during the load application has been introduced in Eq. (3) according to the conventional scalar damage index $\kappa = 1 - E/E_0$, where E is the secant stiffness at the end of loading and E_0 is the initial tangent stiffness. Usually damage index κ is about 0.10–0.15 or 0.22–0.35 for low ($0.35f_{cm}(t)$) or medium ($0.55f_{cm}(t)$) applied stress levels, respectively.

$$\varepsilon'_{cr}=\varepsilon'_{bc}+\varepsilon'_{dc} \tag{6}$$

$$\varepsilon'_{bc}=\left[17.5(c+w)^{2.0}(w/c)^{2.4}\left\{\ln(t')\right\}^{-0.67}\right]\times10^{-10} \tag{7}$$

$$\varepsilon'_{dc}=\left[\frac{4500(w/c)^{4.2}(c+w)^{1.4}}{\left[\ln\left(\frac{v/s}{10}\right)\right]^{-2.2}\left\{1-\frac{RH}{100}\right\}^{0.36}t_0^{-0.30}}\right]\times10^{-10} \tag{8}$$

B) For the high strength SCC with range of applicability by using Eq. (3-5):

$45\%\le RH\le 90\%$; $120kg/m^3\le w\le 230kg/m^3$;

$100mm\le v/s\le 300mm$; $0.30\le w/c\le 0.65$;

$55\le f_{c,28d}\le 100MPa$; $260kg/m^3\le c\le 500kg/m^3$.

$$\varepsilon'_{cc}(t,t',t_0)=\sigma'_{cp}\times\left[\frac{4w(1-RH/100)+350}{12+f'_c(t')}\ln(t-t'+1)\right]\times(10\times(c/p)^{0.678}) \quad for \quad c/p<0.65 \tag{9}$$

$$\varepsilon'_{cc}(t,t',t_0)=\sigma'_{cp}\times\left[\frac{4w(1-RH/100)+350}{12+f'_c(t')}\ln(t-t'+1)\right]\times(13\times(c/p)^{0.701}) \quad for \quad c/p<0.65 \tag{10}$$

where for t_0, t' and t is replaced by:

$$t=\sum_{i=1}^{n}\Delta t_i\exp\left[13.65-\frac{4000}{273+T(\Delta t_i)/T_0}\right]$$

Table 10 Summary of factors accounted for by different prediction models.

	Models	CEB-FIP (2010)	ACI 209R (1997)	Eurocode 2 (2004)	JSCE (2002)	AASHTO (2004)	AASHTO (2007)	AS 3600 (2009)
Intrinsic Factors	Aggregate Type							
	A/C Ratio							
	Air Content		■					■
	Cement Content	■		■	■			
	Cement Type							
	Concrete Density		■					■
	Fine/Total Aggregate Ratio (Mass)		■					■
	Slump		■					■
	w/c Ratio				■			
	Water Content				■			
Extrinsic Factors	Age at First Loading	■	■	■	■	■	■	■
	Age of Sample				■			
	Applied Stress	■	■	■	■			■
	Characteristic Strength at Loading							
	Cross-section Shape				■			
	Curing Conditions							
	Compressive Strength at 28 Days	■	■	■	■	■	■	■
	Duration of Load	■	■	■	■			■
	Effective Thickness	■	■	■	■	■	■	■
	Elastic Modulus at Age of Loading							
	Elastic Modulus at 28 Days	■	■	■	■			■
	Relative Humidity	■	■	■	■	■	■	■
	Temperature				■			
	Time Drying Commences							

Table 11 Coefficient of correlation factor (R^2) of creep prediction models for CC and SCC.

Creep prediction models	CC	SCC
	R^2	R^2
CEB-FIP (2010)	0.41	0.58
ACI 209R (1997)	0.79	0.84
Eurocode 2 (2004)	0.89	0.80
JSCE (2002)	0.89	0.87
AASHTO (2004)	0.86	0.87
AASHTO (2007)	0.90	0.80

Table 12 Coefficient of correlation factor (R^2) of shrinkage prediction models for CC and SCC.

Shrinkage prediction models	CC	SCC
	R^2	R^2
CEB-FIP (2010)	0.70	0.57
ACI 209R (1997)	0.62	0.66
Eurocode 2 (2004)	0.72	0.55
JSCE (2002)	0.84	0.83
AASHTO (2004)	0.42	0.47
AASHTO (2007)	0.88	0.86
AS 3600 (2009)	0.65	0.80

5.4 Proposed shrinkage model

The comparison of the different models and the experimental database shows that ACI 209R (1997), JSCE (2002) and AASHTO (2004) models have conservative drying shrinkage predictions. In this study, based on required certain intrinsic and/or extrinsic variables for SCC, JSCE (2002) drying shrinkage model gives the best approximation of the drying shrinkage strain. Therefore, with the JSCE (2002) model as a basis, it is tried to formulate some suggestions to include the cement-to-powder (c/p) ratio into the formulas in order to obtain a better prediction of the time-dependent deformations of normal strength and high strength of SCC. These results are showed into Eq. (11) to Eq. (23).

For the normal strength SCC (with range of applicability same as creep proposed model):

$$\varepsilon'_{cr}\left(t,t_0\right)=\varepsilon'_{sh}\left[\,1-\exp\left\{-0.1\left(t-t_0\right)^{(-2.4(c/p)+2.3)}\right\}\right] \tag{11}$$

$$\varepsilon'_{sh}=\begin{bmatrix}-50+78\left\{1-\exp\left(\dfrac{RH}{100}\right)\right\}+38.3\ \ln w\\ -0.92\ln\left(\dfrac{w}{c}\right)-5\left[\ln\left(\dfrac{v/s}{10}\right)\right]^2\end{bmatrix}\times\left(10^{-5}\right) \tag{12}$$

for c/p ≥ 0.65

$$\varepsilon'_{sh}=\begin{bmatrix}-50+78\left\{1-\exp\left(\dfrac{RH}{100}\right)\right\}+37.5\ \ln w\\ -0.92\ln\left(\dfrac{w}{c}\right)-5\left[\ln\left(\dfrac{v/s}{10}\right)\right]^2\end{bmatrix}\times\left(10^{-5}\right) \tag{13}$$

for c/p ≥ 0.65

For the high strength SCC with range of applicability (with range of applicability same as creep proposed model):

$$\varepsilon'_{cs}\ \left(t,t_0\right)=\ \varepsilon'_{ds}\ \left(t,t_0\right)+\varepsilon'_{as}\ \left(t,t_0\right) \tag{14}$$

$$\varepsilon'_{ds}\ \left(t,t_0\right)=\frac{\varepsilon'_{ds\infty}\ \left(t-t_0\right)}{\beta+\ \left(t-t_0\right)} \tag{15}$$

$$\varepsilon'_{ds\infty}=\frac{\varepsilon'_{ds\rho}}{\eta\ t_0}\ \left(\times10^{-6}\right) \tag{16}$$

$$\varepsilon'_{ds\rho}=\left[\frac{\alpha\left(1-RH/100\right)w}{1+110\ \exp\left\{-\dfrac{400}{f'_{c,28d}}\right\}}\right]\times\left(0.015+1.35\ (c/p)\right)^{-1} \tag{17}$$

for c/p<0.65

$$\varepsilon'_{ds\rho}=\left[\frac{\alpha\left(1-RH/100\right)w}{1+110\ \exp\left\{-\dfrac{410}{f'_{c,28d}}\right\}}\right]\times\left(0.015+1.05\ (c/p)\right)^{-1} \tag{18}$$

for c/p ≥ 0.65

Table 13 Variations of *a* and *b* constants with w/c ratio.

w/c	*a*	*b*
0.20	1.2	0.4
0.23	1.5	0.4
0.30	0.6	0.5
0.40	0.1	0.7
≥0.50	0.03	0.8

$$\beta=\frac{4\ w\sqrt{v/s}}{100+0.7\ t_0} \tag{19}$$

$$\eta=\left[\ 15\ \exp\left(0.007\ f'_c(28)\right)+0.25\ w\ \right]\times10^{-4} \tag{20}$$

$$\varepsilon'_{as}\left(t,t_0\right)=\ \varepsilon'_{as}\left(t\right)-\varepsilon'_{as}\left(t_0\right) \tag{21}$$

$$\varepsilon'_{as}\ \left(t\right)=\gamma\ \varepsilon'_{as\infty}\left[\ 1-\exp\left\{-a\ \left(t-t_s\right)^b\right\}\ \right]\times10^{-6} \tag{22}$$

$$\varepsilon'_{as\infty}=3070\exp\left\{-7.2\left(w/c\right)\right\} \tag{23}$$

$\alpha = 11$ for normal and low heat cement or $\alpha = 15$ for high early strength cement. where, for t_0, t' and t is replaced by the temperature adjusted concrete age and γ is a coefficient representing the influence of the cement and admixtures type (maybe 1 when only ordinary Portland cement is used). The variations of *a* and *b* constants with w/c ratio are given in **Table 13**.

6. Discussion of the proposed models

Proposed creep and shrinkage models are useable for lower and higher c/p and are adjusted to the normal and high strength SCC. In creep model non-linear creep amplification function (Eq. (3)) is added to the creep model that shown influential stress function on the creep behavior. The proposed creep model is adjusted to normal and high strength SCC. Furthermore, SCC loading age parameter is included in the creep model as Eq. (5).

But, before to analyze the predictability of the proposed models it is important to inform that although shrinkage and creep are not totally independent phenomena (Neville, 1983; Bažant, 1994; Reinhardt, 2006), in this experimental program, the total strain was roughly understood as being composed by the addition of these independent phenomena. Consequently, experimental results of creep strain used to verify the predictability of the proposed creep model were determined as the difference between the total strain and shrinkage strain (Leemann, 2011, Reinhardt, 2006, CEB-FIB, 2010). Besides, according to the experimental data reported above, the following parameters were considered in the predictability of the proposed models: RH, w, c, w/c, v/s, c/p and $f'_{cd,28d}$ that are clear from the experimental program.

Figure 4 shows comparison of the proposed creep model with the available experimental results of creep. Analyzing the **Fig. 4** one observes that the proposed

model provide an accurate prediction. In fact, most of the creep results predicted by the proposed model were slightly overestimated but always with a difference lower than 10% to the experimental results. As shown in the **Fig. 4**, the proposed creep model provided better prediction of creep data for SCC mixture with a coefficient of correlation factor (R^2) of 0.93, 0.95, 0.92 and 0.91 compared to N-SCC, D-SCC, S-SCC, and DS-SCC experimental results.

In terms of the proposed shrinkage model, **Fig. 5** shows a comparison of the SCC shrinkage from experimental results versus calculated values from proposed model for (a) N-SCC, (b) D-SCC, (c) S-SCC, and (d) DS-SCC mixes. Observing **Fig. 5**, roughly speaking, one notes that the proposed model provided a good prediction. The predicted results were mostly conservative (especially after the age of 300 days), the maximum difference (10%) between predicted and experimental results. As shown in the **Fig. 5**, the proposed shrinkage model provided better prediction of creep data for SCC mixture with a coefficient of correlation factor (R^2) of 0.91, 0.93, 0.90 and 0.89 compared to N-SCC, D-SCC, S-SCC, and DS-SCC experimental results.

7. Conclusions

The predictability of deformation models have been investigated for CC and SCC in this paper. Two new models are proposed for an accurate prediction of creep and shrinkage for concrete structures made with HSSCC. Based on comparisons between different models and on comparisons to the experimental results, the following conclusions can be drawn from this study:

- For the CC mixtures the AASHTO (2007) and JSCE (2002) models provided better predictions of the creep and shrinkage data compared to the other models. Although the Eurocode 2 (2004) and AASHTO (2004) models had provided suitable predictions for creep they were not so successfully for shrinkage.
- For the SCC mixtures the JSCE (2002) model provided better predictions of the creep and shrinkage data compared to the other models because of the certain intrinsic and/or extrinsic variables. The AASHTO (2004) and ACI 209R (1992) CC models provided also suitable predictions for creep and the AASHTO (2007) and AS 3600 (2009) CC models provided also suitable predictions for shrinkage.

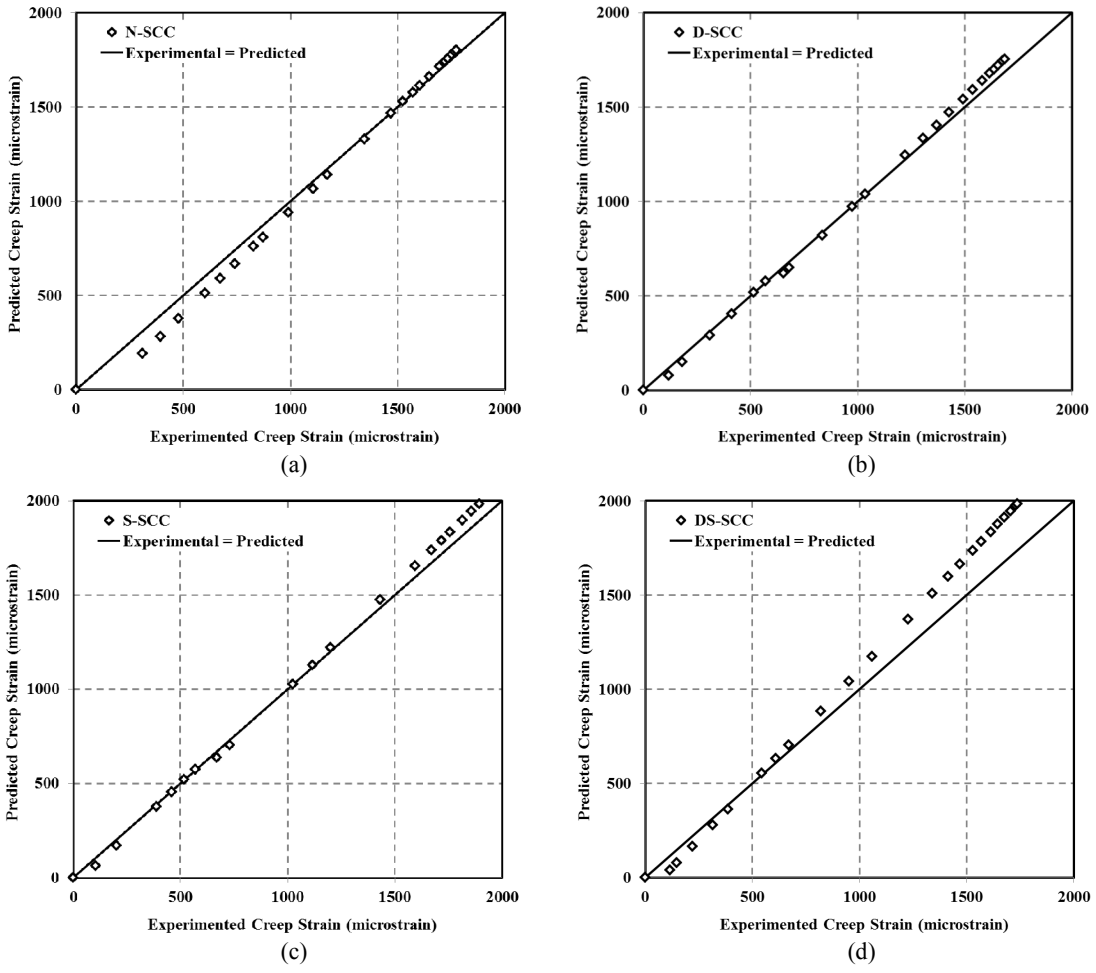

Fig. 4 Comparison of the SCC creep from experimental results versus calculated values from proposed model for (a) N-SCC, (b) D-SCC, (c) S-SCC, and (d) DS-SCC mixes.

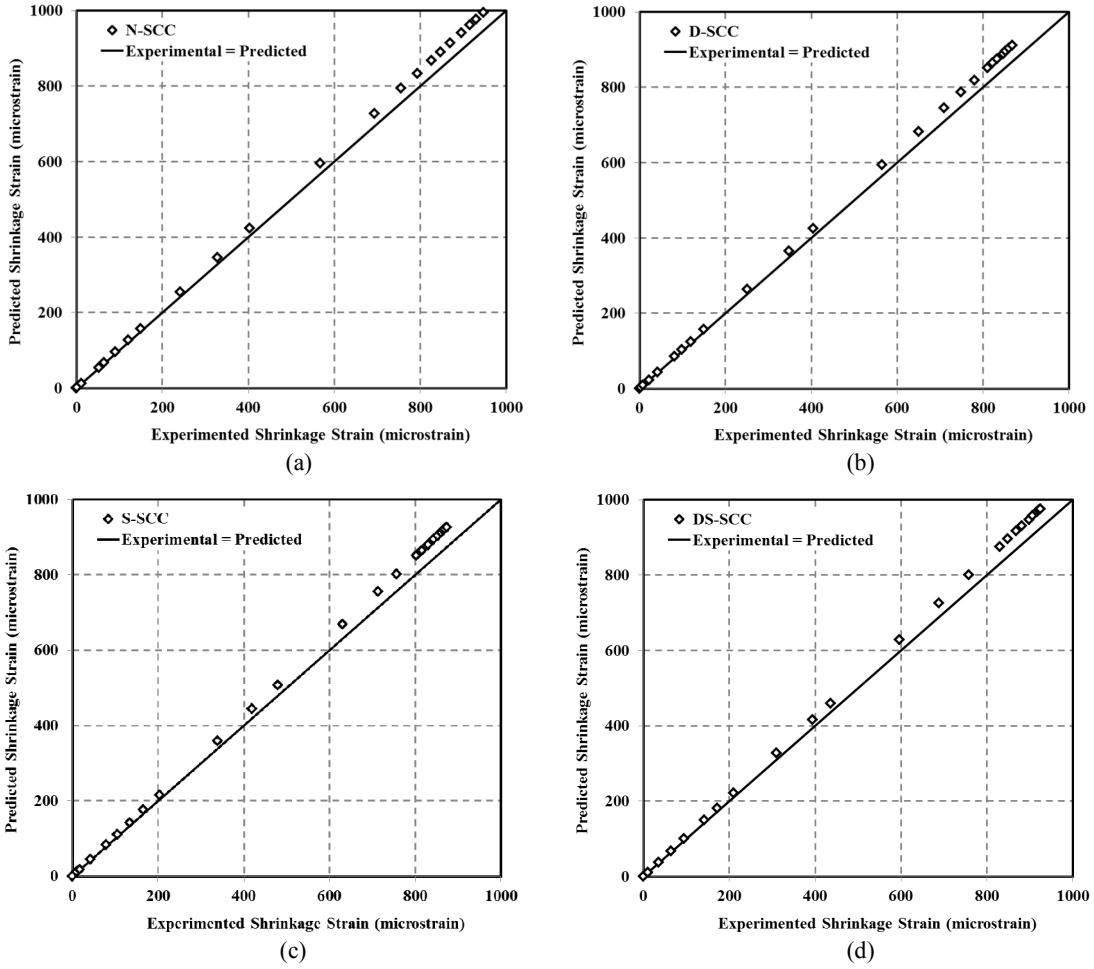

Fig. 5 Comparison of the SCC shrinkage from experimental results versus calculated values from proposed model for (a) N-SCC, (b) D-SCC, (c) S-SCC, and (d) DS-SCC mixes.

- The proposed creep and shrinkage models have good predictions high strength the SCC mixtures. The comparison between the predicted values and the experimental results conducted in this study showed that the proposed models were able to predict creep and shrinkage with high accuracy.

References

AASHTO (2004). "Bridge design specifications and commentary." American Association of Highway and Transportation Officials (AASHTO), Washington, D.C.

AASHTO (2007). "Interim bridge design specifications and commentary." American Association of Highway and Transportation Officials (AASHTO), Washington, D.C.

ACI Committee 209, (1994). "Prediction of creep, shrinkage, and temperature effects in concrete structures." ACI 209R-92, American Concrete Institute, Farmington Hills, Michigan.

ACI 209R, (1997). "Prediction of creep, shrinkage, and temperature effects in concrete structures." ACI 209R-92, American Concrete Institute, Farmington Hills, Michigan.

AC1 232.2R-03, (2004). "Use of Fly Ash in Concrete." ACI Committee 232.

ACI 233R-95, (2000). "*Ground granulated blast-furnace slag as a cementitious constituent in concrete*." ACI Committee 233.

ACI 237R-07, (2007). "*Self-consolidating concrete*." ACI Committee 237.

AS 1012.13, (1992). "*Determination of the drying shrinkage of concrete for samples prepared in the field or in the laboratory*." Standards Australia.

AS 1012.14, (1991). "*Method for securing and testing from hardened concrete for compressive strength*." Standards Australia.

AS 1012.16, (1996). "*Determination of creep of concrete cylinders in compression*." Standards Australia.

AS 1012.17, (1997). "*Determination of the static chord modulus of elasticity and Poisson's ratio of concrete specimens*." Standards Australia.

AS 1141, (2011). "*Methods for sampling and testing aggregates - Particle size distribution - Sieving method*." Standards Australia.

AS 1478.1, (2000). "*Chemical admixtures for concrete, mortar and grout - Admixtures for concrete*."

Standards Australia.
AS 2350, (2006). "*Methods of testing portland and blended cements*." Standards Australia.
AS 3582.2, (2001). "*Supplementary cementitious materials for use with portland and blended cement - Slag - Ground granulated iron blast-furnace*." Standards Australia.
AS 3583, (1998). "*Methods of test for supplementary cementitious materials for use with portland cement.*" Standards Australia.
AS 3600, (2009). "*Concrete structures*." Australian Standards.
AS 3972, (2010). "*General purpose and blended cements*." Standards Australia.
Aslani, F. and Nejadi, S., (2013). "Mechanical characteristics of self-compacting concrete with and without fibers." *Magazine of Concrete Research*, 65(10), 608–622.
Aslani, F. and Nejadi, S., (2012a). "Mechanical properties of conventional and self-compacting concrete: An analytical study." *Construction and Building Materials*, 36, 330-347.
Aslani, F. and Nejadi, S., (2012b). "Bond characteristics of steel fibre reinforced self-compacting concrete." *Canadian Journal of Civil Engineering*, 39(7), 834-848.
Aslani, F. and Nejadi, S., (2011a). "Comparison of creep prediction models for self-compacting and conventional concrete." *In*: Khrapko, M and Wallevik, O. eds., *9th International Symposium on High Performance Concrete*, Rotorua, New Zealand, August 2011, New Zealand Concrete Society, New Zealand, 1-10.
Aslani, F. and Nejadi, S., (2011b). "Comparison of shrinkage prediction models for self-Compacting and Conventional Concrete." *In*: Khrapko, M and Wallevik, O. eds., *9th International Symposium on High Performance Concrete*, Rotorua, New Zealand, August 2011, New Zealand Concrete Society, New Zealand, 1-10.
ASTM standards, (2000). Volume 04.02, Concrete and aggregates.
ASTM C31-11b, (2000). "*Standard test methods for sampling and testing fly ash or natural pozzolans for use in portland-cement concrete*." ASTM standards 2000 (Annual book).
ASTM C183-08, (2000). "*Standard practice for sampling and the amount of testing of hydraulic cement*." ASTM standards 2000 (Annual book).
ASTM C989-06, (2000). "*Standard specification for ground granulated blast-furnace slag for use in concrete and mortars*." ASTM standards 2000 (Annual book).
ASTM C1077-13, (2000). "*Standard practice for agencies testing concrete and concrete aggregates for use in construction and criteria for testing agency evaluation*." ASTM standards 2000 (Annual book).
Bažant, Z., Huet, C. and Müller, H., (1994). "Comment on recent analysis of concrete creep linearity and applicability of principle of superposition." *Materials and Structures*, 27(6), 359-361.
Bhattacharya, A., (2008). "*Effects of aggregate grading and admixtures/fillers on fresh and hardened properties of self-consolidating concrete*." MSc Thesis, West Virginia University.
CEB-FIP, (1990). "*High-strength concrete state of the art report*." Thomas Telford, London.
Chopin, D., Francy, O., Lebourgeois, S. and Rougeau, P., (2003). "Creep and shrinkage of heat-cured self-compacting concrete (SCC)." *3rd International Symposium on Self-Compacting Concrete*, Reykjavik, Iceland, 672-683.
Cordoba, B., (2007). "*Creep and shrinkage of self-consolidating concrete* (*SCC*)." MSc Thesis, University of Wyoming.
European guidelines, (2005). "*The European guidelines for self-compacting concrete*."
Eurocode 2, (2004). "*European standard EN 1992-1: Design of concrete structures. Part 1: General rules and Rules for Buildings*."
Heirman, G., Vandewalle, L., Van Gemerta, D., Boel, V., Audenaert, K., De Schutter, G., Desmetd, B. and Vantomme, J., (2008). "Time-dependent deformations of limestone powder type self-compacting concrete." *Engineering Structures*, 3, 2945-2956.
Horta, A., (2005). "*Evaluation of self-consolidating concrete for bridge structures applications*." MSc Thesis, Georgia Institute of Technology.
Güneyisi, E., Gesoğlu, M. and Özbay, E., (2010). "Strength and drying shrinkage properties of self-compacting concretes incorporating multi-system blended mineral admixtures." *Construction and Building Materials*, 24, 1878-1887.
Issa, M., Alhassan, M., Shabila, H. and Krozel, J., (2005). "Laboratory performance evaluation of self-consolidating concrete." *Proceeding of the Second North American Conference on the Des. and Use of Self Consolidating Concrete and the Fourth Int. RILEM Symposium on Self-Consolidating Concrete*, Center for Advanced Cement-Based Materials (ACBM), Chicago, 857-862.
JSCE, (2002). "*Standard specifications for concrete structure-2002*."
Khayat, K. H. and Long, W. J., (2010). "Shrinkage of precast, prestressed self-consolidating concrete." *ACI Materials Journal*, 107(3), 231-238.
Kim, Y. H., (2008). "*Characterization of self-consolidating concrete for the design of precast, pretensioned bridge superstructure elements*." PhD Thesis, Texas A&M University.
Larson, K., (2006). "*Evaluation the time-dependent deformation and bond characteristics of a self-consolidating concrete mix and the implication for pretensioned bridge applications*." PhD Thesis, Kansas State University.
Leemann, A., Lura, P. and Loser, R., (2011). "Shrinkage

and creep of SCC - The influence of paste volume and binder composition." *Construction and Building Materials*, 25(5), 2283-2289.

Loser, R. and Leemann, A., (2009). "Shrinkage and restrained shrinkage cracking of self-compacting concrete compared to conventionally vibrated concrete." *Materials and Structures*, 42, 71-82.

Ma, K., Xie, Y., Long, G. and Luo, Y., (2009). "Drying shrinkage of medium strength SCC." *Second International Symposium on Design, Performance and Use of Self-Consolidating Concrete SCC'2099*, China, 657-663.

Naito, C. J., Parent, G. and Brunn, G., (2006). "Performance of bulb-tee girders made with self-consolidating concrete." *PCI Journal*, 51(6), 72-85.

Neville, A. M., Dilger, W. H. and Brooks, J. J., (1983). "*Creep of plain and structural concrete.*" London New York: Construction Press.

Neville, A. M., (1996). "*Properties of concrete*." 4th Ed., New York: John Wiley and Sons, Inc.

Oliva, M. G. and Cramer, S., (2008). "*Self-consolidating concrete: Creep and Shrinkage Characteristics*." Report, University of Wisconsin.

Persson, B., (2001). "A comparison between mechanical properties of SCC and the corresponding properties of normal concrete." *Cement and Concrete Research*, 31(2), 193-198.

Persson, B., (2005). "Creep of self-compacting concrete." *Proc. Int. Conf., CONCREEP 7*, Nantes, 535-540.

Poppe, A. M. and De Schutter, G., (2001). "Creep and shrinkage of self-compacting concrete." *Proocedings of the Sixth International Conference CONCREEP-6*, 563-568.

Reinhardt, H.-W. and Rinder, T., (2006). "Tensile creep of high-strength concrete." *Journal of Advanced Concrete Technology*, 4(2), 277-283.

RTA (Regional Transportation Authority). (2006). "*Materials test methods*." Vol. 1.

Schindler, A. K., Barnes, R. W., Roberts, J. B. and Rodriguez, S., (2007). "Properties of self-consolidating concrete for prestressed members." *ACI Material Journal*, 104(1), 53-61.

Turcry, P., Loukili, A., Haidar, K., Pijaudier-Cabot, G. and Belarbi, A., (2006). "Cracking tendency of self-compacting concrete subjected to restrained shrinkage: Experimental study and modelling." *ASCE, Journal of materials in civil engineering*, 18(1), 46-54.

Zheng, J., Chao, P. and Luo, S., (2009). "Experimental study on factors influencing creep of self-compacting concrete." *Second International Symposium on Design, Performance and Use of Self-Consolidating Concrete, SCC'2009*, China, 703-709.

Notation

w = water
c = cement
v/s = volume to surface ratio
w/c = water to cement ratio
c/p = cement to powder ratio
f'_c = compressive strength
$f'_{cm}(t)$ = mean value of compressive strength at time t
$f'_{c,28d}$ = compressive strength at the age of 28 days
RH = relative humidity (%)
t_0, t' and t = effective age (days) of concrete at the beginning of drying, at the beginning of loading, and during loading respectively
σ'_{cp} = creep stress unit
μ, λ and α = parameters to be obtained from a least square minimization procedure
s' and n = parameters that have to be specifically calibrated for each SCC concrete mix by using experimental results
κ = is a conventional scalar damage index
ε'_{sh} = final value of shrinkage strain
$\varepsilon'_{cs}(t,t_0)$ = shrinkage strain of concrete from age to t
$\varepsilon'_{ds}(t,t_0)$ = drying shrinkage strain of concrete from age to t
ε'_{dsp} = the final value of drying shrinkage strain
$\varepsilon'_{ds\infty}$ = final value of drying shrinkage
$\varepsilon'_{sc}(t,t_0)$ = shrinkage strain of concrete from age of t_0 to t
$\varepsilon'_{as}(t,t_0)$ = autogenous shrinkage strain of concrete from the start of setting to age t
$\varepsilon'_{as\infty}$ = final value of autogenous shrinkage strain
ε'_{cr} = final value of creep strain per unit stress
ε'_{bc} = final value of basic creep strain per unit stress
ε'_{dc} = final value of drying creep strain per unit stress
$\varepsilon'_{cc}(t,t',t_0)$ = creep strain
α = coefficient representing the influence of the cement type
β = represents time dependency of drying shrinkage
γ = coefficient representing the influence of the cement and admixtures type (γ may be 1 when only ordinary Portland cement is used)
η = constant related to compressive strength and water content
t = is the temperature adjusted concrete age,
t_0 = starting drying concrete age,
a and b = constants
Δt_i = the number of days where the temperature T prevails
$T(\Delta t_i)$ = the temperature (°C) during the time period Δt_i
T_0 = 1 °C